Journal of Applied Mathematics and Computing (2023) 69:3245–3260
https://doi.org/10.1007/s12190-023-01877-5

ORIGINAL RESEARCH

Dynamics of a fractional COVID-19 model with immunity using harmonic incidence mean-type

Nandhini Mohankumar[1] · **Lavanya Rajagopal**[1]

Received: 11 January 2023 / Revised: 28 March 2023 / Accepted: 7 May 2023 /
Published online: 31 May 2023

Abstract
The transmission dynamics of COVID-19 is investigated through the prism of the Atangana-Baleanu fractional model with acquired immunity. Harmonic incidence mean-type aims to drive exposed and infected populations towards extinction in a finite time frame. The reproduction number is calculated based on the next-generation matrix. A disease-free equilibrium point can be achieved globally using the Castillo-Chavez approach. Using the additive compound matrix approach, the global stability of endemic equilibrium can be demonstrated. Utilizing Pontryagin's maximum principle, we introduce three control variables to obtain the optimal control strategies. Laplace transform allows simulating the fractional-order derivatives analytically. Analysis of the graphical results led to a better understanding of the transmission dynamics.

Keywords COVID-19 · Reproduction number · Immunity · Harmonic incidence mean-type

Mathematics Subject Classification 34A08 · 34D23 · 49K15

1 Introduction

The global SARS-CoV-2 pandemic caused substantial death tolls, along with significant economic and personal damage. Despite the widespread transmission of the

R. Lavanya author contributed equally to this work.

✉ Lavanya Rajagopal
lavnya.gopal@gmail.com

Nandhini Mohankumar
nandhinimohankumar@gmail.com

[1] Department of Mathematics, Coimbatore Institute of Technology, Civil Aerodrome (PO), Coimbatore, Tamilnadu 641014, India

disease and the existence of asymptomatic carriers, the development of new variants has had an extreme impact on the health of the worldwide population [16]. Several factors contribute to the spread of the virus, including variations, diminishing antibody levels, and its inability to be taken down. COVID-19 vaccines have proven very effective in preventing this outbreak from progressing [11]. In the long run, an effective COVID-19 vaccine will stimulate a strong, durable, adaptive immune response, and this vaccine-driven immunity is referred to as adaptive immunity [17]. Innate immunity is another type of immunity that develops upon pathogen exposure. In response to an infection, the immune system attempts to destroy the infectious pathogen, leaving traces and allowing the system to produce antibodies sufficient to protect the body [15]. The immune system can develop by vaccination and prior infection, but neither is efficient [5].

Numerous mathematical models are being used to determine the probability of the spread of infectious diseases [6]. The dynamic system with fractional-order derivatives provides a means to describe the genetic properties and effectiveness of the memory involved in various biological systems [13]. Models based on fractional-order are better at capturing infectious diseases dynamics than other models. Fractional order differential equation models provide a deeper insight into the study of the disease [14]. The harmonic incidence allows extinguishing the infected and exposed population rapidly. The harmonic mean is less prone to errors than geometric and arithmetic means. Over time, the harmonic incidence rate suggests that infected cases are likely to become extinct. It may be easier to achieve more quickly than other incidence rates [2].

After the spread of the COVID-19, a few fraction models have emerged to model the dynamics. In [23], the authors proposed the Atangana-Baleanu fraction model in Caputo sense, the existence and uniqueness of the model is investigated using Picard-Lindel method and numerical simulations are performed. In [27], a generalized fractional-order SEIR model is proposed. In particular, the fractional model under consideration has a good predictive ability for the next two weeks of epidemics. Numerical simulations of COVID-19 fractional-order modeling have been conducted in [28], for Wuhan (China). Simulating the Caputo-Fabrizio fractional-order derivative has been carried out using the Adams-Bashforth numerical scheme.

In [9], Isa Abdillahi et.al., have examined the dynamics of COVID-19 variants using Caputo-Fabrizio fractional derivatives. The authors have demonstrated that the variant with the largest reproduction number will dominate the other variant. Padmapriya et.al., have developed a model using Caputo fractional derivative to predict the dynamics of COVID-19 and the study is used to check the applications of the fractional derivative in uncertainty conditions [20]. The present work extends the model proposed in [18] to study the dynamics of COVID-19 with harmonic incidence mean-type. This research work aims to propose a fractional model with a harmonic incidence mean rate to reduce the exposed and infected population. To drive the exposed and infected population to extinction, the incidence rate is incorporated into the transmission. To the best of our knowledge, the harmonic incidence mean rate has not been considered for two transmission rates while formulating fractional models.

This paper is organized as follows, the model analysis that includes reproduction number and equilibrium points in Sect. 2. In Sect. 3, the model stability is determined

using Castilla Chavez approach. In Sect. 4, according to Pontryagin's maximum principle, we analyze the optimal control by incorporating control variables. By utilizing the Laplace transforms, the numerical simulation is examined for the fractional-order model, the results are presented in Sect. 5.

2 Model analysis

Caputo and Riemann-Lioville fractional operators are the most well-known fractional operators. When these operators are employed to study the structure of models, they may prevent better findings due to their singularity quality. To overcome these drawbacks, Caputo and Fabrizio created a non-singular fractional operator known as the Caputo-Fabrizio derivative, which has an exponential kernal function. Atangana and Baleanu recently proposed another form of the non-singular derivative that makes use of the non-singular kernel function called Atangana-Baleanu fractional derivative (AB) [1]. As one of the most recent and generalized fractional operators, the Atangana-Baleanu derivative has a non-local and non-singular kernel. In other words, kernels determine convergence; if kernels are singular, convergence will not be achieved. As a result, the AB kernel describes complexity in a easy and comprehensive manner. In this section, the AB fractional derivative model in Caputo sense for COVID-19 transmission dynamics with acquired immunity by both past COVID-19 infection and vaccination is proposed. The preliminary results of the Atangana-Baleanu fractional derivatives [21] are considered to develop the model. The model is divided into 5 compartments susceptible $S_c(t)$, exposed $E_c(t)$, infected $I_c(t)$, treatment $T_c(t)$ and recovered $R_c(t)$ classes. Here we introduce the harmonic mean type incidence rate for two transmission terms between the susceptible and exposed, infected classes.

$$
\begin{aligned}
{}^{ABC}D_t^{\alpha} S_c(t) &= R + V - \beta_1 \left[\frac{2\, S_c(t)E_c(t)}{S_c(t)+E_c(t)}\right] - \beta_2 \left[\frac{2\, S_c(t)I_c(t)}{S_c(t)+I_c(t)}\right] - \mu S_c(t) \\
&\quad + \rho R_c(t), \\
{}^{ABC}D_t^{\alpha} E_c(t) &= \beta_1 \left[\frac{2\, S_c(t)E_c(t)}{S_c(t)+E_c(t)}\right] + \beta_2 \left[\frac{2\, S_c(t)I_c(t)}{S_c(t)+I_c(t)}\right] - (\sigma + \kappa + \mu)E_c(t), \\
{}^{ABC}D_t^{\alpha} I_c(t) &= (\sigma + \kappa)E_c(t) - (\eta + d + \mu)I_c(t), \\
{}^{ABC}D_t^{\alpha} T_c(t) &= \eta I_c(t) - (\gamma + \mu)T_c(t), \\
{}^{ABC}D_t^{\alpha} R_c(t) &= \gamma T_c(t) - (\mu + \rho)R_c(t).
\end{aligned} \tag{1}
$$

with initial conditions $S_c(0) = S_{c_0}, E_c(0) = E_{c_0}, I_c(0) = I_{c_0}, T_c(0) = T_{c_0}, R_c(0) = R_{c_0}$, where R is the recruitment rate of susceptible people, V is the recruitment rate of vaccinated people, β_1 is the transmission rate of infection transferred from exposed individuals to susceptible humans, β_2 is the transmission rate of infection transferred from infected persons to susceptible persons, σ is the rate of susceptible individuals got exposed to infection, η is the rate of individuals getting treatment after knowing symptoms, μ is the natural death rate, γ is the recovery rate, d is the disease-induced death rate, ρ is the rate of people who are recovered from COVID-19 gets susceptible to infection with acquired immunity, κ is the rate of infection development in the exposed population with acquired immunity, $(\kappa < \sigma)$.

2.1 Reproduction number

The infected functional equations are considered of (1) to obtain the reproduction number. The Jacobian matrix of infected equations are decomposed as F and V matrices and the spectral radius of the FV^{-1} is

$$R_0 = \frac{2(\sigma+\kappa)[\beta_1(\gamma+\mu)+\beta_2\eta]}{(\sigma+\kappa+\mu)(\eta+d+\mu)(\gamma+\mu)}.$$

2.2 Equilibrium points

The disease-free equilibrium point (DFE) $E_0 = \{S_{c_0}, E_{c_0}, I_{c_0}, T_{c_0}, R_{c_0}\} = \left\{\frac{R+V}{\mu}, 0, 0, 0, 0\right\}$ and the endemic equilibrium point (EEP) $E_* = \{S_c{}^*, E_c{}^*, I_c{}^*, T_c{}^*, R_c{}^*\}$, where

$$\begin{aligned}
S_c{}^* &= \frac{1}{\mu}\left\{\left[\frac{\rho\gamma\eta}{(\gamma+\mu)(\mu+\rho)} - \frac{(\sigma+\kappa+\mu)(\eta+d+\mu)}{(\sigma+\kappa)}\right] I_c{}^* + R + V\right\},\\
E_c{}^* &= \frac{(\eta+d+\mu)I_c{}^*}{(\sigma+\kappa)},\\
T_c{}^* &= \frac{\eta I_c{}^*}{\gamma+\mu},\\
R_c{}^* &= \frac{\gamma\eta I_c{}^*}{(\gamma+\mu)(\mu+\rho)}.
\end{aligned}$$

3 Stability analysis

In this section, we establish the global stability of DFE, E_0 and EEP, E^*.

3.1 Global stability of equilibrium points

The Castillo-Chavez approach [25] aims to achieve the global stability of the DFE point.

Theorem 3.1 *The DFE E_0 of the model (1) is locally asymptotically stable when $R_0 < 1$ and unstable otherwise.*

Proof We have to prove the following conditions to show that the global stability of the disease-free equilibrium using Castillo Chavez method.

- If $\frac{d\chi_1}{dt} = G(\chi_1, 0)$, then χ_1^0 is globally asymptotically stable.
- $H(\chi_1, \chi_2) = B\chi_2 - \bar{H}(\chi_1, \chi_2)$, where $\bar{H}(\chi_1, \chi_2) \geq 0$ for $(\chi_1, \chi_2) \in \Delta$

Let $\chi_1 = (S_c, R_c)$, $\chi_2 = (E_c, I_c, T_c)$ and define $E_0 = (\chi_1^0, 0)$ where $\chi_1^0 = \frac{R+V}{\mu}$. By the model (1),

$$\frac{d\chi_1}{dt} = \begin{bmatrix} R + V - \beta_1 \left(\frac{2S_c(t)E_c(t)}{S_c(t)+E_c(t)}\right) - \beta_2 \left(\frac{2S_c(t)I_c(t)}{S_c(t)+I_c(t)}\right) - \mu S_c(t) + \rho R_c(t) \\ \gamma T_c(t) - (\mu + \rho) R_c(t), \end{bmatrix}$$

with $S_c = S_{c_0}$, $R_c = R_{c_0}$ and $G(\chi_1, 0) = 0$, we have

$$G(\chi_1, 0) = (R + V - \mu S_c), \tag{2}$$

From (2), we have $\chi_1 \to \chi_1^0$ as $t \to \infty$. The first condition has been proved. Now,

$$B\chi_2 - \bar{H}(\chi_1, \chi_2) = \begin{bmatrix} 2\beta_1 - (\sigma + \kappa + \mu) & 2\beta_2 & 0 \\ \sigma + \kappa & -(\eta + d + \mu) & 0 \\ 0 & \eta & -(\gamma + \mu) \end{bmatrix} - \begin{bmatrix} 2\beta_1 E_c - \frac{2\beta_1 S_c E_c}{S_c + E_c} + 2\beta_2 I_c - \frac{2\beta_2 S_c I_c}{S_c + I_c} \\ 0 \\ 0 \end{bmatrix},$$

so that $\left(\frac{2\beta_1 E_c(S_c+E_c)-2\beta_1 S_c E_c}{S_c+E_c}\right) = \frac{2\beta_1 E_c^2}{S_c+E_c} \geq 0$ and $\left(\frac{2\beta_2 I_c(S_c+I_c)-2\beta_2 S_c I_c}{S_c+I_c}\right) = \frac{2\beta_2 I_c^2}{S_c+I_c} \geq 0$

Thus, $\bar{H}(\chi_1, \chi_2)$ is positive definite and B is an M-matrix. Hence both the conditions of Castillo-Chavez have been proved. □

Theorem 3.2 *The equilibrium point E^* of the model (1) is globally asymptotically stable when $R_0 > 1$ and unstable otherwise.*

Proof The Jacobian matrix of the sub-system is

$$\begin{bmatrix} \frac{2\beta_1 S_c^* E_c^*}{(S_c^*+E_c^*)^2} - \frac{2\beta_1 E_c^*}{S_c^*+E_c^*} + \frac{2\beta_2 S_c^* I_c^*}{(S_c^*+I_c^*)^2} - \frac{2\beta_2 I_c^*}{S_c^*+I_c^*} - \mu & \frac{2\beta_1 S_c^* E_c^*}{(S_c^*+E_c^*)^2} - \frac{2\beta_1 S_c^*}{S_c^*+E_c^*} \\ \frac{2\beta_1 E_c^*}{S_c^*+E_c^*} - \frac{2\beta_1 S_c^* E_c^*}{(S_c^*+E_c^*)^2} + \frac{2\beta_2 I_c^*}{S_c^*+I_c^*} - \frac{2\beta_2 S_c^* I_c^*}{(S_c^*+I_c^*)^2} & \frac{2\beta_1 S_c^*}{S_c^*+E_c^*} - \frac{2\beta_1 S_c^* E_c^*}{(S_c^*+E_c^*)^2} - \sigma - \kappa - \mu \\ 0 & \sigma + \kappa \\ 0 & 0 \end{bmatrix} \begin{bmatrix} \frac{2\beta_2 S_c^* I_c^*}{(S_c^*+I_c^*)^2} - \frac{2\beta_2 S_c^*}{S_c^*+I_c^*} & 0 \\ \frac{2\beta_2 S_c^*}{S_c^*+I_c^*} - \frac{2\beta_2 S_c^* I_c^*}{(S_c^*+I_c^*)^2} & 0 \\ -\eta - d - \mu & 0 \\ \eta & -\gamma - \mu \end{bmatrix}, \tag{3}$$

$$J^{[3]} = \begin{bmatrix} A_{11} & 0 & 0 & 0 \\ \eta & A_{22} & \frac{2\beta_2 S_c^*}{S_c^*+I_c^*} - \frac{2\beta_2 S_c^* I_c^*}{(S_c^*+I_c^*)^2} & \frac{2\beta_2 S_c^*}{S_c^*+I_c^*} - \frac{2\beta_2 S_c^* I_c^*}{(S_c^*+I_c^*)^2} \\ 0 & \sigma + \kappa & A_{33} & -\frac{2\beta_1 S_c^*}{S_c^*+E_c^*} + \frac{2\beta_1 S_c^* E_c^*}{(S_c^*+E_c^*)^2} \\ 0 & 0 & \frac{2\beta_1 E_c^*}{S_c^*+E_c^*} - \frac{2\beta_1 S_c^* E_c^*}{(S_c^*+E_c^*)^2} + \frac{2\beta_2 I_c^*}{S_c^*+I_c^*} - \frac{2\beta_2 S_c^* I_c^*}{(S_c^*+I_c^*)^2} & A_{44} \end{bmatrix},$$

where,

$$A_{11} = -\left(\frac{2\beta_1 E_c^*}{S_c^* + E_c^*} + \frac{2\beta_2 I_c^*}{S_c^* I_c^*} - \frac{2\beta_2 S_c^* I_c^*}{(S_c^* + I_c^*)^2} - \frac{2\beta_1 S_c^*}{S_c^* + E_c^*} + \sigma + \kappa + \eta + d + 3\mu\right),$$

$$A_{22} = -\left(\frac{2\beta_1 E_c^*}{S_c^* + E_c^*} + \frac{2\beta_2 I_c^*}{S_c^* + I_c^*} - \frac{2\beta_2 S_c^* I_c^*}{(S_c^* + I_c^*)^2} - \frac{2\beta_1 S_c^*}{S_c^* + E_c^*} + \sigma + \kappa + \gamma + 3\mu\right),$$
$$A_{33} = -\left(\frac{2\beta_1 E_c^*}{S_c^* + E_c^*} - \frac{2\beta_1 S_c^* E_c^*}{(S_c^* + E_c^*)^2} + \frac{2\beta_2 I_c^*}{S_c^* + I_c^*} - \frac{2\beta_2 S_c^* I_c^*}{(S_c^* + I_c^*)^2} + \eta + d + \gamma + 3\mu\right),$$
$$A_{44} = -\left(\frac{2\beta_1 S_c^* E_c^*}{(S_c^* + E_c^*)^2} - \frac{2\beta_1 S_c^*}{S_c^* + E_c^*} + \sigma + \kappa + \eta + d + \gamma + 3\mu\right),$$

The function $P(\chi) = P(S_c, E_c, I_c, T_c) = diag(S_c, E_c, I_c, T_c)$ and we have,

$$P^{-1}(\chi) = diag\left\{\frac{1}{S_c}, \frac{1}{E_c}, \frac{1}{I_c}, \frac{1}{T_c}\right\},$$

By direct calculation, we have

$$B = P_f P^{-1} + P J^{|3|} P^{-1},$$
$$P J^{|3|} P^{-1} = \begin{bmatrix} m_{11} & 0 & 0 & 0 \\ m_{21} & m_{22} & m_{23} & m_{24} \\ 0 & m_{32} & m_{33} & m_{34} \\ 0 & 0 & m_{43} & m_{44} \end{bmatrix},$$

where

$$m_{11} = \frac{\dot{S}_c}{S_c} - \left(\frac{2\beta_1 E_c^*}{S_c^* + E_c^*} + \frac{2\beta_2 I_c^*}{S_c^* + I_c^*} - \frac{2\beta_1 S_c^*}{S_c^* + E_c^*} - \frac{2\beta_2 S_c^* I_c^*}{(S_c^* + I_c^*)^2} + \sigma + \kappa + \eta + d + 3\mu\right),$$
$$m_{21} = \frac{E_c}{S_c}\eta,$$
$$m_{22} = \frac{\dot{E}_c}{E_c} - \left(\frac{2\beta_1 E_c^*}{S_c^* + E_c^*} + \frac{2\beta_2 I_c^*}{S_c^* + I_c^*} - \frac{2\beta_2 S_c^* I_c^*}{(S_c^* + I_c^*)^2} - \frac{2\beta_1 S_c^*}{S_c^* + E_c^*} + \sigma + \kappa + \gamma + 3\mu\right),$$
$$m_{23} = \frac{E_c}{I_c}\left(\frac{2\beta_2 S_c^*}{S_c^* + I_c^*} - \frac{2\beta_2 S_c^* I_c^*}{(S_c^* + I_c^*)^2}\right),$$
$$m_{24} = \frac{E_c}{T_c}\left(\frac{2\beta_2 S_c^*}{S_c^* + I_c^*} - \frac{2\beta_2 S_c^* I_c^*}{(S_c^* + I_c^*)^2}\right),$$
$$m_{32} = \frac{I_c}{E_c}(\sigma + \kappa),$$
$$m_{33} = \frac{\dot{I}_c}{I_c} - \left(\frac{2\beta_1 E_c^*}{S_c^* + E_c^*} + \frac{2\beta_2 I_c^*}{S_c^* + I_c^*} - \frac{2\beta_1 S_c^* E_c^*}{(S_c^* + E_c^*)^2} - \frac{2\beta_2 S_c^* I_c^*}{(S_c^* + I_c^*)^2} + \eta + d + \gamma + 3\mu\right),$$
$$m_{34} = \frac{I_c}{T_c}\left(\frac{2\beta_1 S_c^* E_c^*}{(S_c^* + E_c^*)^2} - \frac{2\beta_1 S_c^*}{S_c^* + E_c^*}\right),$$
$$m_{43} = \frac{T_c}{I_c}\left(\frac{2\beta_1 E_c^*}{S_c^* + E_c^*} - \frac{2\beta_1 S_c^* E_c^*}{(S_c^* + E_c^*)^2} + \frac{2\beta_2 I_c^*}{S_c^* + I_c^*} - \frac{2\beta_2 S_c^* I_c^*}{(S_c^* + I_c^*)^2}\right),$$
$$m_{44} = \frac{\dot{T}_c}{T_c} - \left(\frac{2\beta_1 S_c^* E_c^*}{(S_c^* + E_c^*)^2} - \frac{2\beta_1 S_c^*}{S_c^* + E_c^*} + \sigma + \kappa + \eta + d + \gamma + 3\mu\right).$$

We define the Lozinski measure $\mu(B)$ where $\mu(B) = h_i, i = 1, 2, 3, 4$ [12]. By taking the limit $t \to \infty$ the integration of $\mu(B)$ takes the following form,

$$\lim_{t\to\infty} sup\frac{1}{t}\int_0^t h_1(t)dt \leq -(\sigma+\kappa+\eta+d+3\mu),$$
$$\lim_{t\to\infty} sup\frac{1}{t}\int_0^t h_2(t)dt \leq -(\sigma+\kappa+\gamma+3\mu),$$
$$\lim_{t\to\infty} sup\frac{1}{t}\int_0^t h_3(t)dt \leq -(\eta+d+\gamma+3\mu),$$
$$\lim_{t\to\infty} sup\frac{1}{t}\int_0^t h_4(t)dt \leq -(\sigma+\kappa+\eta+d+\gamma+3\mu). \tag{4}$$

The combining equation of (4) is,

$$\bar{q} = \lim_{t\to\infty} supsup\frac{1}{t}\int_0^t \mu(B)dt < 0. \tag{5}$$

From (5), the considered subsystem is globally asymptotically stable around the equilibrium point ($S_c{}^*$, $E_c{}^*$, $I_c{}^*$, $T_c{}^*$). The remaining system of the model (1) is R_c. When $R_c \to R_c{}^*$ as $t \to \infty$. Hence, the proof. □

4 Optimal control

The control strategy for our model relies on the optimal control theory. Our study derives the necessary conditions based on Pontryagin's maximum principle [7] to identify the possible optimal control of the proposed epidemic model. As a result, the model (1) is reformulated using control interventions as

$$\begin{aligned}
{}^{ABC}D_t^{\alpha} S_c(t) &= R + V - \beta_1(1-u_1)\left[\frac{2\,S_c(t)E_c(t)}{S_c(t)+E_c(t)}\right] - \beta_2(1-u_1)\left[\frac{2\,S_c(t)I_c(t)}{S_c(t)+I_c(t)}\right] \\
&\quad - \mu S_c(t) + \rho R_c(t) - u_2 S_c(t), \\
{}^{ABC}D_t^{\alpha} E_c(t) &= \beta_1(1-u_1)\left[\frac{2\,S_c(t)E_c(t)}{S_c(t)+E_c(t)}\right] + \beta_2(1-u_1)\left[\frac{2\,S_c(t)I_c(t)}{S_c(t)+I_c(t)}\right] \\
&\quad - (\sigma+\kappa+\mu)E_c(t), \\
{}^{ABC}D_t^{\alpha} I_c(t) &= (\sigma+\kappa)E_c(t) - (\eta+d+\mu+u_3)I_c(t), \\
{}^{ABC}D_t^{\alpha} T_c(t) &= (\eta+u_3)I_c(t) - (\gamma+\mu)T_c(t), \\
{}^{ABC}D_t^{\alpha} R_c(t) &= \gamma T_c(t) - (\mu+\rho)R_c(t).
\end{aligned} \tag{6}$$

with $S_c(0) \geq 0$, $E_c(0) \geq 0$, $I_c(0) \geq 0$, $T_c(0) \geq 0$, $R_c(0) \geq 0$, where u_1 is the media control like awareness campaigns like TV ads and sticker campaigns, u_2 is the vaccination control like encouraging the public to get fully vaccinated, u_3 is the IPC priorities control, a practice of preventing the spread of infections by identifying them quickly, isolating them immediately, and ensuring their safe management. The control objective functional associated with the model is

$$J[u_1,u_2,u_3] = \int_0^T \left[b_1E_c(t) + b_2I_c(t) + b_3T_c(t) + \frac{c_1u_1^2(t)}{2} + \frac{c_2u_2^2(t)}{2} + \frac{c_3u_3^2(t)}{2}\right]dt, \tag{7}$$

where c_i is used to balance the control factors and b_i is the positive weights. Let us define the Hamiltonian condition to derive the optimality conditions by considering (6) and (7),

$$\bar{H} = L[E_c, I_c, T_c, u_1, u_2, u_3] + \lambda_1 S_c(t) + \lambda_2 E_c(t) + \lambda_3 I_c(t) + \lambda_4 T_c(t) + \lambda_5 R_c(t). \quad (8)$$

where $\lambda_1, \lambda_2, \lambda_3, \lambda_4, \lambda_5$ are the adjoint variables. Accordingly, the optimal control $u^*(t) = (u_1{}^*, u_2{}^*, u_3{}^*)$ of the model, that minimizes the objective functional (7) is characterized by

$$\begin{aligned}
u_1{}^*(t) &= max\left[min\left(\frac{1}{c_1}\left\{(\lambda_2 - \lambda_1)\frac{2\beta_1 S_c E_c}{S_c + E_c} + (\lambda_2 - \lambda_1)\frac{2\beta_2 S_c I_c}{S_c + I_c}\right\}, 0\right), 1\right],\\
u_2{}^*(t) &= max\left[min\left(\frac{1}{c_2}\{\lambda_1 S_c\}, 0\right), 1\right],\\
u_3{}^*(t) &= max\left[min\left(\frac{1}{c_3}\{(\lambda_3 - \lambda_4) I_c\}, 0\right), 1\right]. \quad (9)
\end{aligned}$$

The optimality system of the model (6) and the fractional derivative adjoint equation with the characterization of the optimal control (9) represents the analytical solution of the optimal control.

5 Numerical simulation

Consider the model,

$$\begin{aligned}
{}_0^{ABC}D_t^{\alpha} S_c(t) &= G_1(t, S_c(t)),\\
{}_0^{ABC}D_t^{\alpha} E_c(t) &= G_2(t, E_c(t)),\\
{}_0^{ABC}D_t^{\alpha} I_c(t) &= G_3(t, I_c(t)),\\
{}_0^{ABC}D_t^{\alpha} T_c(t) &= G_4(t, T_c(t)),\\
{}_0^{ABC}D_t^{\alpha} R_c(t) &= G_5(t, R_c(t)). \quad (10)
\end{aligned}$$

After some manipulation, the series solution is given by $S_c = \sum_{n=0}^{\infty} S_{c_n}$, $E_c = \sum_{n=0}^{\infty} E_{c_n}$, $I_c = \sum_{n=0}^{\infty} I_{c_n}$, $T_c = \sum_{n=0}^{\infty} T_{c_n}$, $R_c = \sum_{n=0}^{\infty} R_{c_n}$. The recursive formula using the initial conditions are given by,

$$\begin{aligned}
S_{c_{n+1}}(t) &= S_{c_n(0)} + L^{-1}\\
&\left[\left(\frac{s^{\alpha}(1-\alpha)+\alpha}{s^{\alpha}(F(\alpha))}\right) L\left\{R + V - \beta_1\left[\frac{2S_c E_c}{S_c + E_c}\right] - \beta_2\left[\frac{2S_c I_c}{S_c + I_c}\right] - \mu S_c + \rho R_c\right\}\right],\\
E_{c_{n+1}}(t) &= E_{c_n(0)} + L^{-1}\\
&\left[\left(\frac{s^{\alpha}(1-\alpha)+\alpha}{s^{\alpha}(F(\alpha))}\right) L\left\{\beta_1\left[\frac{2S_c E_c}{S_c + E_c}\right] + \beta_2\left[\frac{2S_c I_c}{S_c + I_c}\right] - (\sigma + \kappa + \mu) E_c\right\}\right],\\
I_{c_{n+1}}(t) &= I_{c_n(0)} + L^{-1}\left[\left(\frac{s^{\alpha}(1-\alpha)+\alpha}{s^{\alpha}(F(\alpha))}\right) L\{(\sigma + \kappa) E_c - (\eta + d + \mu) I_c\}\right],
\end{aligned}$$

Table 1 Parameter lists and their values

Parameter	Values	Source
R	0.5	Assumed
V	0.0001	Assumed
β_1	0.9567	[29]
β_2	0.3567	[8]
ρ	0.01	[3]
σ	0.21	[10]
κ	0.007	[19]
η	0.07	[22]
d	0.018	[4]
μ	0.062	[26]
γ	0.9833	[24]

$$T_{c_{n+1}}(t) = T_{c_n(0)} + L^{-1}\left[\left(\frac{s^{\alpha}(1-\alpha)+\alpha}{s^{\alpha}(F(\alpha))}\right) L\left\{\eta I_c - (\gamma+\mu)T_c\right\}\right],$$
$$R_{c_{n+1}}(t) = R_{c_n(0)} + L^{-1}\left[\left(\frac{s^{\alpha}(1-\alpha)+\alpha}{s^{\alpha}(F(\alpha))}\right) L\left\{\gamma T_c - (\mu+\rho)R_c\right\}\right].$$

where $S_{c_0}(t) = S_c(0), E_{c_0}(t) = E_c(0), I_{c_0}(t) = I_c(0), T_{c_0}(t) = T_c(0), R_{c_0}(t) = R_c(0)$. Therefore, $S_c(t) = \lim_{n\to\infty} S_{c_n}(t), E_c(t) = \lim_{n\to\infty} E_{c_n}(t), I_c(t) = \lim_{n\to\infty} I_{c_n}(t), T_c(t) = \lim_{n\to\infty} T_{c_n}(t), R_c(t) = \lim_{n\to\infty} R_{c_n}(t)$. The graphs are depicted using the parameter values in Table 1.

The fractional model is simulated for different set of parameters using Matlab. Parameter values were taken from Table 1. All parameters are given in daily units. Figure 1, 2, 3, 4, 5 illustrates the dynamic behavior of the susceptible, exposed, infected, treatment, and recovered population for different fractional orders. The main control interventions that are considered in the model are vaccination, the media, and IPC priority controls. These control variables help to decrease the exposed population.

According to Fig. 6, the graph shows that the variation in the susceptible population is sustained in the presence of control, however in the absence of control the number of susceptible population decreases. This finding shows that the control interventions are preventing the disease's transmission and has the ability to maintain the susceptible population.

Figure 7 illustrates that the application of control is efficient in reducing the exposed population, but in the absence of control, the number exposed population increases over time. In Fig. 8, infected individuals decline as control measures are implemented, while they rise when no control measures exist. The infected population is reduced by detecting them fast, isolating them immediately, and guaranteeing their safe management with proper treatment. It can also help to avoid further exposure.

In Fig. 9, one can see that the treatment population increases when controls are applied because of the IPC priority control. By isolating the infected population, the control variable encourages them to seek treatment. In Fig. 10, the graph shows that the recovered population increases to the control interventions. The positive rise is

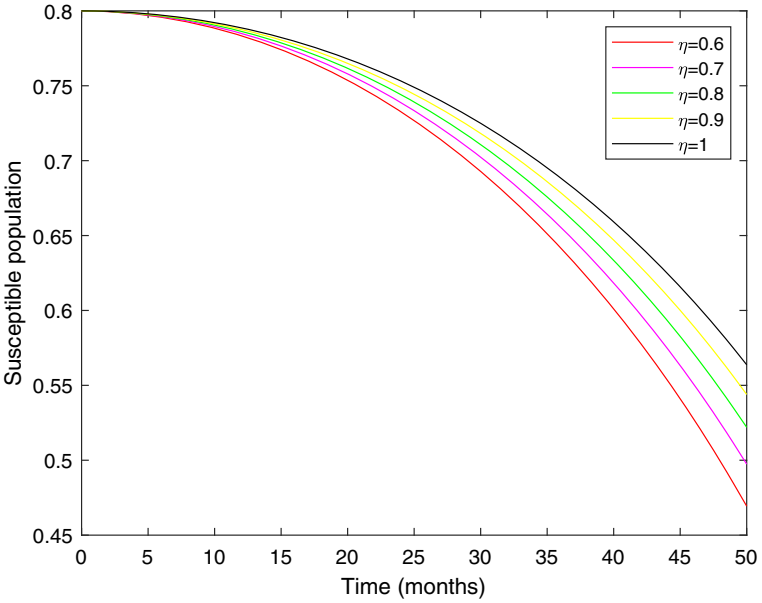

Fig. 1 Graphical reprsentation of susceptible population corresponding to different fractional order

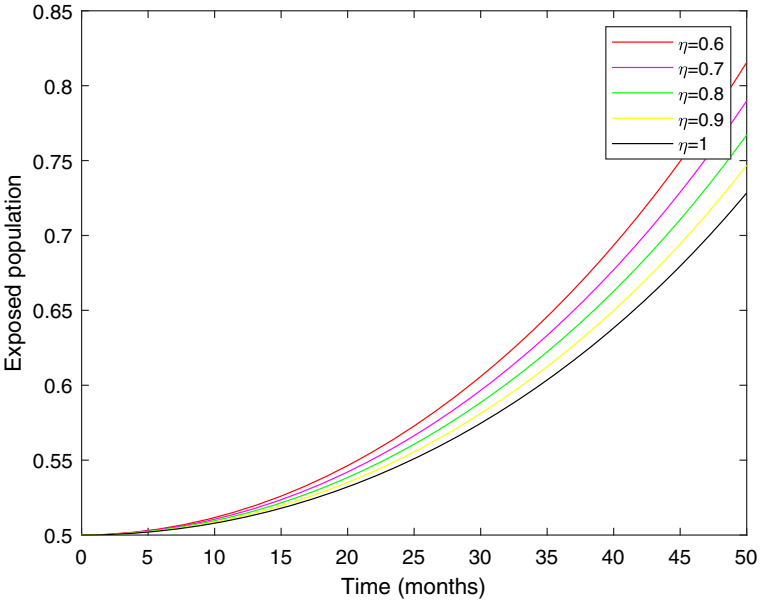

Fig. 2 Graphical reprsentation of exposed population corresponding to different fractional order

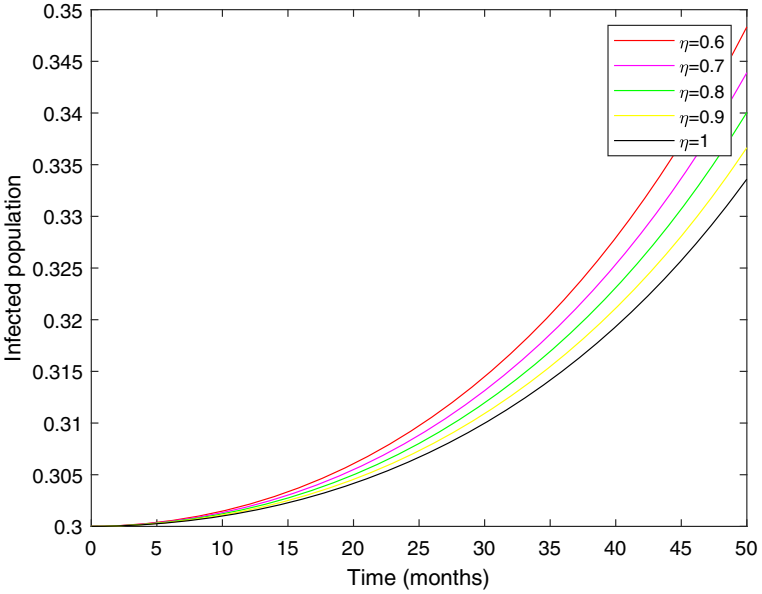

Fig. 3 Graphical reprsentation of infected population corresponding to different fractional order

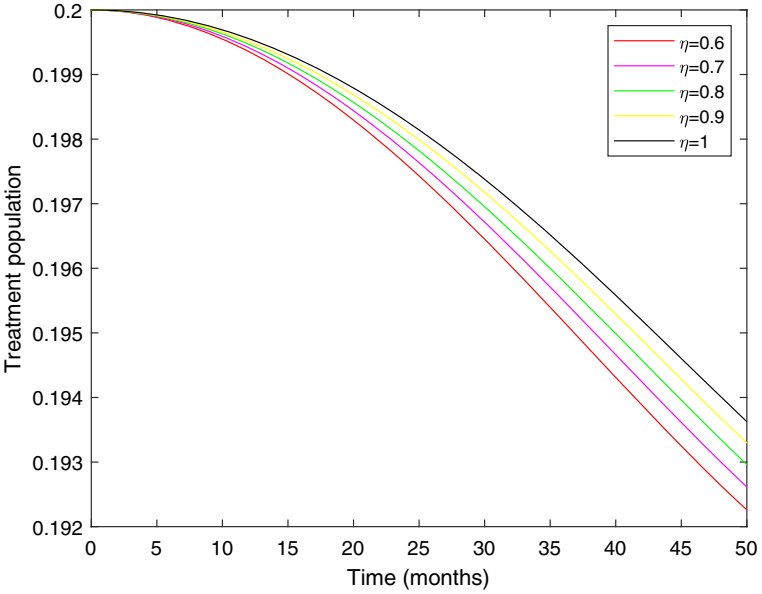

Fig. 4 Graphical reprsentation of treatment population corresponding to different fractional order

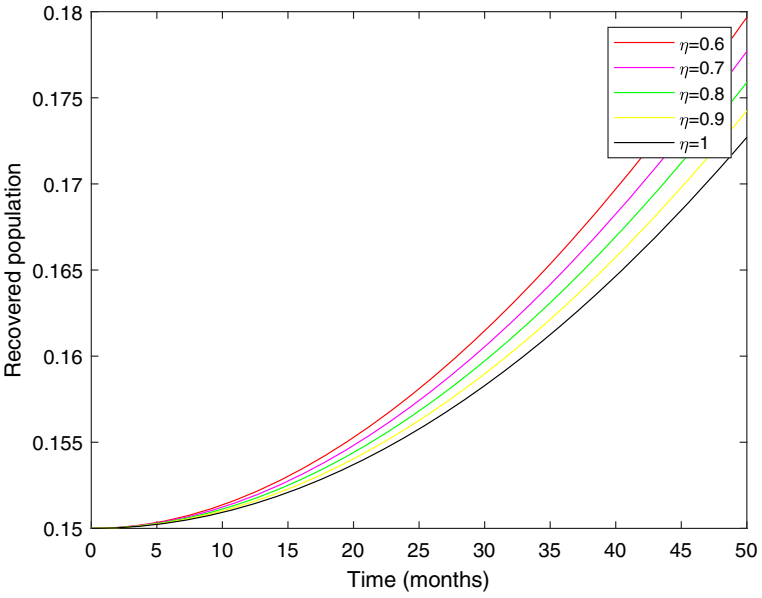

Fig. 5 Graphical reprsentation of recovered population corresponding to different fractional order

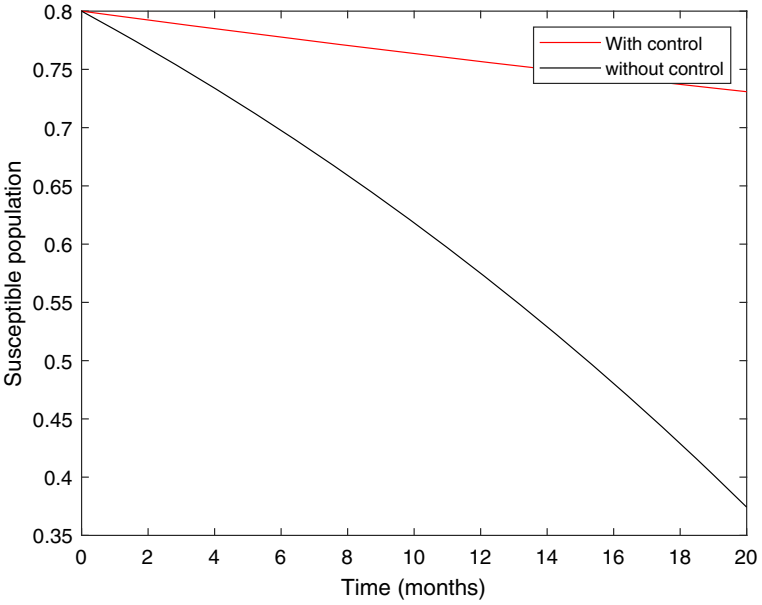

Fig. 6 With and without control interventions in susceptible population

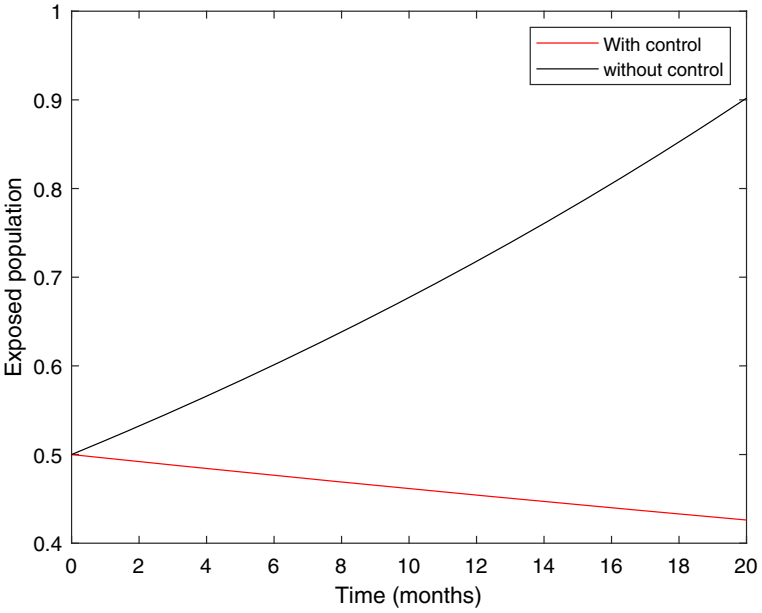

Fig. 7 With and without control interventions in exposed population

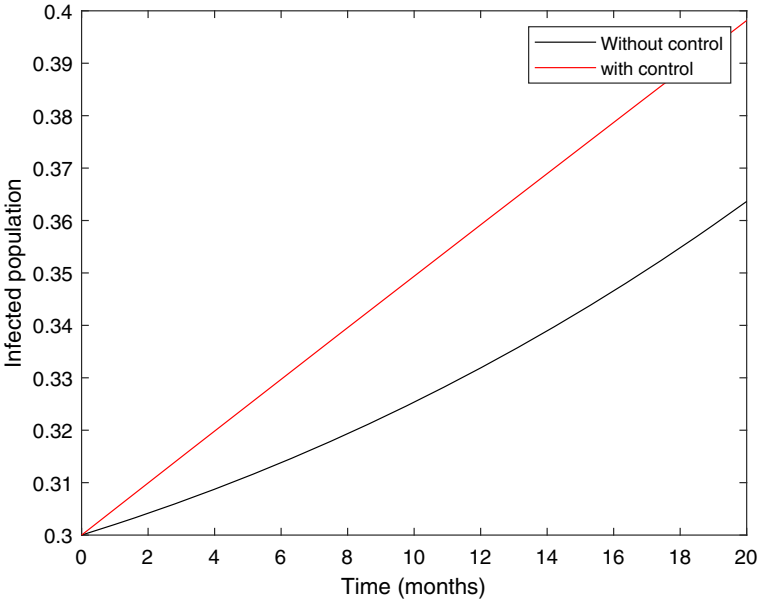

Fig. 8 With and without control interventions in infected population

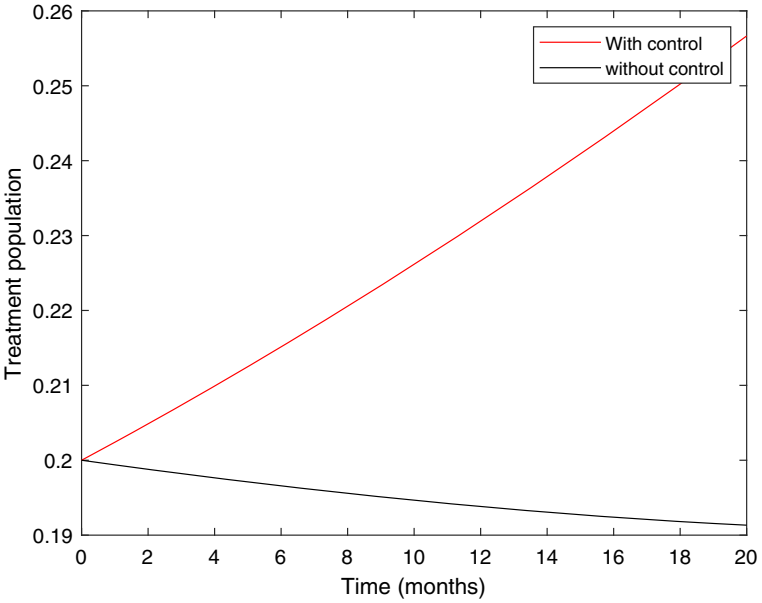

Fig. 9 With and without control interventions in treatment population

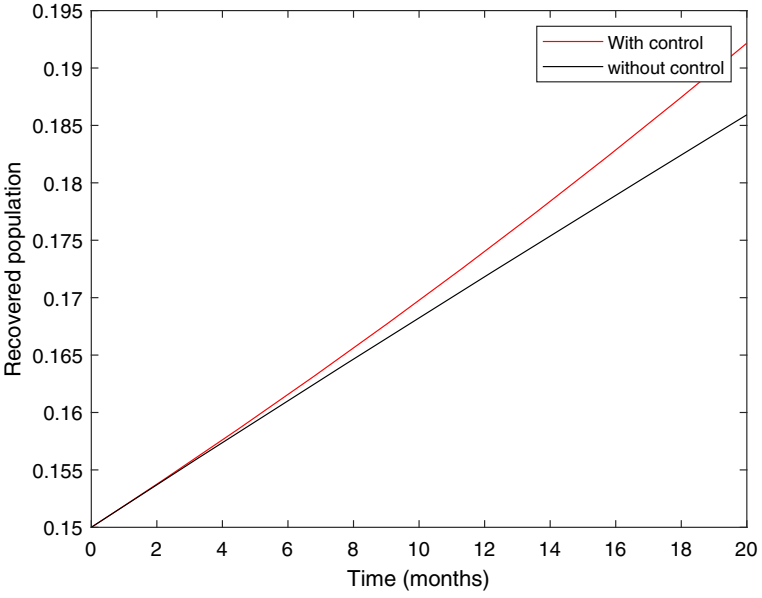

Fig. 10 With and without control interventions in recovered population

attributable to the high infection rates shown in Fig. 8, which resulted in an increase in the recovery compartment.

6 Conclusion

In this paper, we propose a COVID-19 fractional model with acquired immunity. The harmonic mean type incidence is introduced in the model to extinct the exposed and infected cases over time. Using the next-generation matrix, we determine the reproduction number. We studied the global stability of disease-free equilibrium points using the Castillo-Chavez approach and the global stability system of endemic equilibrium points using the third additive compound matrix approach. Pontryagin's maximum principle allows determining the best control strategies with three control variables: media control, vaccination control, and IPC priority control. We simulate fractional-order derivatives analytically using the Laplace transform and illustrate the results graphically. The dynamic behavior of compartments based on fractional order are presented.The combination of control variables impacts the reduction of the exposed population and the rise in vulnerable and recovered cases resulting in an infection-free community.

Declarations

Conflict of interest The authors declare no conflict of interest.

References

1. Atangana, A., Baleanu, D.: New fractional derivatives with non local and Non-singular kernal: theory and Application to Heat transfer model. Therm. Sci. **20**(2), 763–769 (2016)
2. Khan, A., Zarin, R.: Stability analysis of Leishmania epidemic model with harmonic mean type incidence rate. Eur. Phys. J. Plus **135**, 528 (2020)
3. Christian, H.H., Daniela, M.: Assessment of protection against reinfection with SARS-CoV-2 among 4 million PCR-tested individuals in Denmark in 2020: a population-level observational study. The Lancet **397**(10280), 1204–1212 (2021)
4. Diagne, M.L., Rivezaura, H.: A mathematical model of COVID-19 with vaccination and treatment. Comput. Math. Methods Med. **5**, 1250129 (2021)
5. Collins, F.: How immunity generated from COVID-19 vaccines differs from an infection. Science **2**, 859 (2021)
6. Hethcote, H.W.: The mathematics of infectious diseases. Soc. Ind. Appl. Math. Rev. **42**(4), 599–653 (2000)
7. Kheiri, H., Jafari, M.: Otimal control of a fractional-order model for the HIV/AIDS epidemic. Int. J. Bio Math. **11**(7), 1850086 (2018)
8. Isa, A.B., Bashir, A.N.: Optimal control model for the transmission of Novel COVID-19. Comput. Mater. Continua **66**(3), 3089–3106 (2021)
9. Baba, I.A., Rihan, F.A.: A Fractional-order model with different strains of COVID-19. Physica A Stat. Mech. Appl. **603**, 127813 (2022)
10. Koshy, J.: Coronavirus. One in Five Indians Have Been Exposed to Coronavirus, ICMR survey finds, The Hindu (2021)
11. Townsend, J.P., Hassler, H.B.: The durability of immunity against reinfection by SARS-CoV-2: a comparative evolutionary study. The LANCET Microbe **2**(12), e666–e675 (2021)

12. Zhang, J., Jia, J.: Analysis of an SEIR epidemic model with saturated incidence and saturated treatment function. The Sci. World J. **6**, 910421 (2014)
13. Khan, H., Gómez-Aguilar, J.F., Alkhazzan, A., Khan, A.: A fractional order HIV-TB co-infection model with nonsingular Mittag-Leffler law. Math. Methods Appl. Sci. **43**(6), 3786–3806 (2020)
14. Khan, M.A., Ullah, S., Farooq, M.: A new fractional model for tuberculosis with relapse via Atangana-Baleanu derivative. Chaos Solitons Fractals **116**, 227–38 (2018)
15. Thomas, L.: Innate versus adaptive immunity in COVID-19. News Med. Life Sci. **5**, 741 (2021)
16. Johansson, M.A., Quandelacy, T.M.: SARS-CoV-2 transmission from people without COVID-19 symptoms. JAMA Netw. **4**(1), e2035057 (2021)
17. Good, M.F., Hawkes, M.T.: The interaction of Natural and Vaccine-induced immunity with social distancing predicts the evolution of the COVID-19 Pandemic. Clin. Sci. Epidemiol. **11**(5), e02617-20 (2020)
18. Nandhini, M., Lavanya, R., Nieto, J.J.: A fractional COVID-19 model with efficacy of vaccination. Axioms **11**, 446 (2022). https://doi.org/10.3390/axioms11090446
19. Kojima, N., Klausner, J.D.: Protective immunity after recovery from SARS-CoV-2 infection. The Lancet Infect. Dis. **5**, 21 (2021)
20. Kaliyappan, P.V.: Fuzzy fractional mathematical model of COVID-19 epidemic. J. Intell. Fuzzy Syst. **42**, 3299–3321 (2022)
21. Pawar, D.D., Patil, W.D.: Analysis of Malaria dynamics using its fractional order mathematical model. J. Appl. Math. Inform. **39**(1–2), 197–214 (2021)
22. Kaul, R.: COVID-19:7.3 percentage of active cases in ICU's are on ventilators, says centre. India News **2**, 589 (2021)
23. Ullah, R., Wasseem, M.: Analysis of COVID-19 Fractional model pertaining to the Atangana-Baleanu-Caputo fractional derivatives. J. Funct. Spaces **7**, 2643572 (2021)
24. Dutta, S.: India's single-day COVID death toll dips, recovery rate highest since March 2020. Hindustan Times **2**, 96 (2021)
25. Khan, T., Hyo, J.: Classification and sensitivity analysis of the transmission dynamic of hepatitis B. Theoret. Biol. Med. Modell. **14**, 22 (2017)
26. Tamilalagan, P., Krithika, B.: A SEIRUC mathematical model for transmission dynamics of COVID-19, arxiv:2106.08327v1, (2021)
27. Xu, C., Yu, Y., Chen, Y., Lu, Z.: Forecast analysis of the epidemics trend of COVID-19 in the USA by a generalized fractional-order SEIR model. Nonlin. Dyn. **101**, 16211634 (2020)
28. Yadav, R.P., Verma, R.: A numerical simulation of fractional order mathematical modeling of COVID-19 disease in case of Wuhan China. Chaos Solitons Fract **2**, 528 (2020)
29. Shen, Z.-H., Chu, Y.-M.: Mathematical modelling and optimal control of the COVID-19 dynamics. Res. Phys. **31**, 105028 (2021)